

The resulting map (Fig. 1e) shows that the absorption feature has a mean W of 0.2 nm and stretches from roughly north to south across the entire emission line region, corresponding to a length of >30 kpc (the map presents only the area with good signal-to-noise ratio). Its spatial width is rather uncertain, because it is unresolved in the east-west direction ($<1.5''$). It cannot be narrower than $0.5''$ because otherwise even a 100% obscuration would be washed out by our beam into a relative depression of $<25\%$ (0.25 nm). So we assume a projected size of 10×10 kpc² for the absorber, with a deconvoluted equivalent width of about 0.5 nm.

Such an absorber can either consist of one or more clouds located well in front of 4C41.17 (if the blueshift of the absorption is cosmological, the absorber sits at a comoving distance of 5 Mpc). On the other hand, the velocity in the EELR itself is large enough to cover this blueshift; otherwise we would be unable to detect the feature. Thus, a dense, partially ionized cloud at the edge of 4C41.17 could equally explain the absorption. In this latter case more detailed observations are necessary for a physical interpretation. We therefore would like to pursue the former possibility of a physically separated absorber. Such clouds—commonly known as Lyman-forest clouds—and their properties have been extensively studied in the absorption line spectra of high redshift quasars.

For comparison we make use of a spectrum¹⁴ of the quasar Q0000-263 ($z=4.11$), the Lyman-forest of which covers the λ range of our observation. We smoothed the original spectrum (resolution, 0.1 nm) to our instrumental resolution of 1.0 nm. The comparison between smoothed and original spectrum reveals that any absorption feature as deep as that observed in 4C41.17 typically consists of two or more narrow absorption lines. We have to realize therefore, that our 'absorption cloud' is likely to be a superposition of several individual Lyman-forest clouds. Nevertheless, we believe that the outline of the absorber in the W map (Fig. 1e) is most likely to be determined by one single cloud which made the feature strong enough to become detectable, and we assign half of the measured equivalent width (0.25 nm) to this cloud. Assuming a Doppler parameter $b=35$ km s⁻¹ and $N_{\text{H}}/N_{\text{H}^+}=10^{-4}$ as typical for Lyman clouds of that depth (refs 1, 3), we find a column density $N_{\text{H}} \sim 10^{15}$ cm⁻². A cigar-shaped cloud of 40 kpc length and 10 kpc diameter would contain a total hydrogen mass of $\sim 3 \times 10^7 M_{\odot}$.

What is the probability of detecting such an absorption feature in front of 4C41.17? Both the smoothed spectrum of Q0000-263 (ref. 14) and the standard $dN(W, z)/dz$ relation¹⁵ yield ~ 25 features with $W > 0.4$ nm on each line of sight and within one z unit at the observed wavelength. Considering the 'useful' wavelength range of ~ 1.2 nm (the blue half of the width of the emission line) in our search for line features, and the area of the EELR inspected of ~ 20 arcsec², the probability of detecting a cloud of a typical size of a few arcsec² is close to 1.

In conclusion, we believe that we have succeeded in obtaining the first direct observation of a Lyman absorption cloud. Either this cloud belongs directly to the mass concentration around 4C41.17 or it is a physically separated foreground object. In the latter case it would represent the population of Lyman-forest clouds known from the absorption spectra of quasars. In either case, our observations indicate that the relevant absorbers have projected sizes of some 100 kpc² and an elongated shape, like a cigar or a sheet seen almost edge-on in the case of 4C41.17. □

Received 23 September 1992; accepted 19 January 1993.

- Chaffee, F. H., Foltz, C. R., Bechold, J. & Weymann, R. J. *Astrophys. J.* **301**, 116–123 (1986).
- Carwell, R. F., Webb, J. K., Baldwin, J. A. & Atwood, B. *Astrophys. J.* **319**, 709–722 (1987).
- Rauch, M. et al. *Astrophys. J.* **390**, 387–404 (1992).
- Foltz, C. B., Weymann, R. J., Röser, H. J. & Chaffee, F. H. *Astrophys. J.* **281**, L1–L4 (1984).
- Smalley, A. et al. *Astrophys. J.* **389**, 39–52 (1992).
- Tyler, D. *Astrophys. J.* **321**, 69–79 (1987).
- Pettini, M., Hunstead, R. W., Smith, L. J. & Mor, D. P. *Mon. Not. R. astr. Soc.* **246**, 545–564 (1990).
- Ikeuchi, S. in *Dark Matter in the Universe* (eds Sato, H. & Kolama, H.) 50–62 (Springer, Berlin, 1990).

- Spinrad, H. in *Epoch of Galaxy Formation* (eds Frenk, C. S. et al.) 39–56 (Kluwer, Dordrecht, 1988).
- Lilly, S. *Astrophys. J.* **333**, 161–167 (1988).
- Chambers, K. C., Miley, G. K. & van Breugel, W. *Astrophys. J.* **363**, 21–39 (1990).
- Meisenheimer, K. & Hippelein, H. *Astr. Astrophys.* **264**, 455–471 (1992).
- Röser, S. & Bastian, U. *PPM Star Catalogue* (Spektrum Akad., Heidelberg, 1991).
- Webb, J. K. et al. *ESO Messenger* **51**, 15–18 (1988).
- Murdoch, H. S., Hunstead, R. W., Pettini, M. & Blades, J. C. *Astrophys. J.* **309**, 19–32 (1986).

ACKNOWLEDGEMENTS. We thank R. Carswell for the spectrum of Q0000-236 and H. Röser for discussions.

Superconductivity at 94 K in $\text{HgBa}_2\text{CuO}_{4+\delta}$

S. N. Putilin[†]*, E. V. Antipov^{*}, O. Chmaissem[†] & M. Marezio[†]‡

* Chemical Department, Moscow State University, 119899 Moscow, Russia

† Laboratoire de Cristallographie CNRS-UJF, BP 166, 38042 Grenoble Cedex 09, France

‡ AT&T Bell Laboratories, Murray Hill, New Jersey 07974, USA

FOLLOWING the discovery¹ of high-transition-temperature (high- T_c) superconductivity in doped La_2CuO_4 , several families of related compounds have been discovered which have layers of CuO_2 as the essential requirement for superconductivity: the highest transition temperatures so far have been found for thallium-bearing compounds². Recently the mercury-bearing compound $\text{HgBa}_2\text{RCu}_2\text{O}_{6+\delta}$ (Hg-1212) was synthesized³ (where R is a rare-earth element), with a structure similar to the thallium-bearing superconductor $\text{TlBa}_2\text{CaCu}_2\text{O}_7$ (Tl-1212), which has one TlO layer and two CuO_2 layers per unit cell, and a T_c of 85 K (ref. 2). But in spite of its resemblance to Tl-1212, Hg-1212 was found not to be superconducting. Here we report the synthesis of the related compound $\text{HgBa}_2\text{CuO}_{4+\delta}$ (Hg-1201), with only one CuO_2 layer per unit cell, and show that it is superconducting below 94 K. Its structure is similar to that of Tl-1201 (which has a T_c of <10 K)⁴, but its transition temperature is considerably higher. The availability of a material with high T_c but only a single metal oxide (HgO) layer may be important for technological applications, as it seems that a smaller spacing between CuO_2 planes leads to better superconducting properties in a magnetic field⁵.

The samples were prepared by solid state reaction between stoichiometric mixtures of $\text{Ba}_2\text{CuO}_{3+\delta}$ and yellow HgO (98% purity, Aldrich). The precursor $\text{Ba}_2\text{CuO}_{3+\delta}$ was obtained by the same type of reaction between BaO_2 (95% purity, Aldrich) and CuO (NormaPur, Prolabo) at 930 °C in oxygen, according to the procedure described by De Leeuw et al.⁶. The powders were ground in an agate mortar and placed in silica tubes. All these operations were carried out in a dry box. After evacuation, the tubes were sealed, placed in steel containers, as described in ref. 3, and heated for 5 h to reach ~ 800 °C. The samples were then cooled in the furnace, reaching room temperature after ~ 10 h.

The formation of the new phase $\text{HgBa}_2\text{CuO}_{4+\delta}$ was revealed by X-ray powder analysis, performed with a Guinier-Hägg focusing camera and Fe K α radiation (1.93730 Å). Finely powdered silicon ($a=5.43088$ Å at 25 °C) was used as an internal standard. The intensities of the reflections were evaluated by means of an automatic film scanner and indexed on a tetragonal cell with lattice parameters $a=3.8797$ (5) Å, $c=9.509$ (2) Å and assignment $Z=1$. No systematic absences were observed, leading to the number of molecules per unit cell of the space group $P4/mmm$. The c parameter corresponded to the value calculated from the formula $c \approx 9.5 + 3.2(n-1)$, similar to that deduced for the $\text{TlBa}_2\text{R}_{n-1}\text{Cu}_n\text{O}_{2n+3}$ homologous series. We took this as a strong indication that the powder pattern corresponded to that of the first member of the $\text{HgBa}_2\text{R}_{n-1}\text{Cu}_n\text{O}_{2n+2+\delta}$ series.

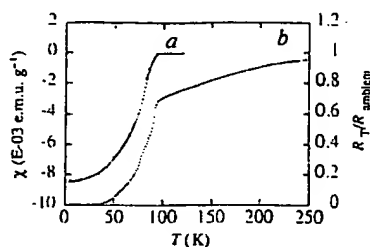


FIG. 1 AC magnetic susceptibility χ (a) and normalized resistivity (b) as a function of temperature for $\text{HgBa}_2\text{CuO}_{4+\delta}$.

Scanning electron microscopy using a JEOL SM 840A equipped with an energy-dispersive spectroscopy (EDS) attachment revealed that the sample was well crystallized with particle sizes of several micrometres. EDS analysis of several well crystallized, flat and oriented grains was performed. Beside Hg, Ba, Cu and O, no other element was detected in the spectra. The average metal ratio found for eight grains was Hg:Ba:Cu = 28(1):47(2):25(1), where the numbers between parentheses are the standard deviations. Determination of the oxygen content by EDS analysis was not possible, so it was estimated by structural analysis and iodometric titration. The cation stoichiometry is in qualitatively good agreement with the proposed formula of the new compound.

Alternating-current magnetic susceptibility measurements between 4.2 and 120 K, done without any additional oxygen treatment, showed that $\text{HgBa}_2\text{CuO}_{4+\delta}$ samples undergo a transition from paramagnetic to diamagnetic with an onset as high as 94 K (Fig. 1a, where the susceptibility is in electromagnetic units g^{-1}). The estimated magnetic susceptibility at 4.2 K. corresponds to >50% of the ideal diamagnetic values.

The resistivity was measured between 4.2 and 250 K by the four-probe technique. The sample was a pressed pellet which was annealed in oxygen for 2 h. The temperature dependence of the normalized resistivity, shown in Fig. 1, exhibits a sharp drop at T_c , but the transition is broad and it reaches the value of zero resistance only at 35 K. This behaviour indicates that the sample is not homogeneous.

To determine the structure of $\text{HgBa}_2\text{CuO}_{4+\delta}$, X-ray powder data were collected by a $\theta/2\theta$ STADI P diffractometer in transmission mode. The experimental conditions were as follows: 2θ range = $6-115^\circ$ (0.02° steps) with fixed counting time 60 s and a rotating sample. An absorption correction was applied and the sample thickness was calculated from the primary beam absorption ($\mu R = 1.7$, where μ is absorption coefficient and R is thickness). The structural refinements were done by the Rietveld method. The initial positional parameters were deduced from a structural model containing the sequence (Hg)(BaO)-(CuO₂)(BaO)(Hg). After convergence (intensity discrepancy factor, $R_1 = 0.039$), a Fourier difference map revealed that the position at $(\frac{1}{2}, \frac{1}{2}, 0)$ of the Hg layer was partially occupied. During the final cycle of refinement, the occupancy factor of a third oxygen atom placed in this position was varied together with the positional and thermal parameters for all atoms (except for the thermal parameter of O(3) which was kept fixed at 1.0 \AA^2). The final intensity (R_1) and profile (R_p) discrepancy factors based on 84 reflections were $R_1 = 0.0367$ and $R_p = 0.116$, with a GOF (goodness of fit) = 0.33.

The final positional and thermal parameters together with the relevant interatomic distances are given in Table 1. Observed, calculated and difference diffraction patterns are shown in Fig. 2. A schematic representation of the structure is shown in Fig. 3. Preliminary structural refinements based on powder neutron diffraction data support the presence of oxygen in the O(3) position with an occupancy factor slightly larger than that found by X-ray powder diffraction data. The neutron data also

TABLE 1 Crystallographic data for $\text{HgBa}_2\text{CuO}_{4+\delta}$

Positional, thermal and occupancy parameters						
Atom	Position	x	y	z	B_{iso} (\AA^2)	Occupancy
Hg	1a	0	0	0	2.55 (5)	1.00
Ba	2h	0.5	0.5	0.2979 (1)	1.43 (4)	1.00
Cu	1b	0	0	0.5	0.88 (9)	1.00
O(1)	2e	0.5	0	0.5	0.4 (3)	1.00
O(2)	2g	0	0	0.206 (2)	2.2 (3)	1.00
O(3)	1c	0.5	0.5	0	1.0	0.10 (3)
Selected interatomic distances (\AA)						
Hg-O(2) ($\times 2$)	1.95 (2)	Cu-O(1) ($\times 4$)	1.940 (1)	Ba-O(1) ($\times 4$)	2.730 (1)	
Hg-O(3)*	2.742 (1)	Cu-O(2) ($\times 2$)	2.79 (2)	Ba-O(2) ($\times 4$)	2.880 (5)	
				Ba-O(3)*	2.831 (1)	

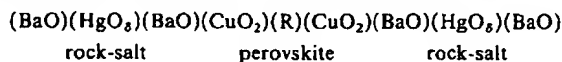
Data obtained using monochromatized $\text{CuK}\alpha_1$ radiation ($\lambda = 1.54056 \text{ \AA}$), giving $a = 3.87768(4) \text{ \AA}$, $c = 9.5073(1) \text{ \AA}$.

* Partially occupied sites.

confirm the large value for the mercury thermal factors. As in the case of the X-ray data, the anisotropic model shows a very slight difference between $B_{11} = B_{22}$ and B_{33} , the thermal factors along x, y and z respectively.

$\text{HgBa}_2\text{CuO}_{4+\delta}$ has a structure related to that of Hg-1212 (ref. 3). Its lattice parameters correspond to four-layered packing along the c-axis of a unit cell: $a = a_{\text{per}}$, $c = 2a_{\text{per}}$ (where a_{per} is the parameter of the perovskite subcell) and its structure contains the sequence (CuO₂)(BaO)(HgO_δ)(BaO)(CuO₂). The Cu cations are octahedrally coordinated, while the coordination of the other cations depends upon the value of δ . This, as obtained from powder X-ray data, is 0.10(3). An important consequence is that most of the Hg cations have two oxygen atoms near them in a 'dumb-bell' configuration, an appropriate coordination for Hg^{2+} cations. Because δ is small and different from zero (within about three standard deviations) X-ray powder data alone are insufficient to determine which sites of the rock-salt positions in the HgO layer are occupied and how they affect the Hg coordination. The extra oxygen atoms are needed in order to increase the average oxidation number of the Cu and to create the concentration of holes necessary for superconductivity. Iodometric titration performed with a large excess of KI leads to 16% of Cu^{3+} , corresponding to $\delta = 0.08$.

Similarly, the structure of $\text{HgBa}_2\text{RCu}_2\text{O}_{6+\delta}$ (the second member of the $\text{HgBa}_2\text{R}_{n-1}\text{Cu}_n\text{O}_{2n+2+\delta}$ series) can be described as six-layered blocks made of rock-salt and perovskite-type structures. In the structure of Hg-1212 the layer sequence is:



The CuO₂ monolayer in Hg-1201 has been replaced by the (CuO₂)(R)(CuO₂) block. As a consequence the Cu cations are

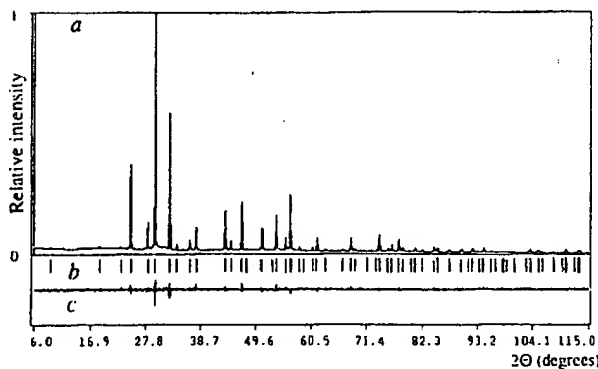


FIG. 2 Observed (a), calculated (b) and difference (c) powder patterns after Rietveld refinement for $\text{HgBa}_2\text{CuO}_{4+\delta}$.

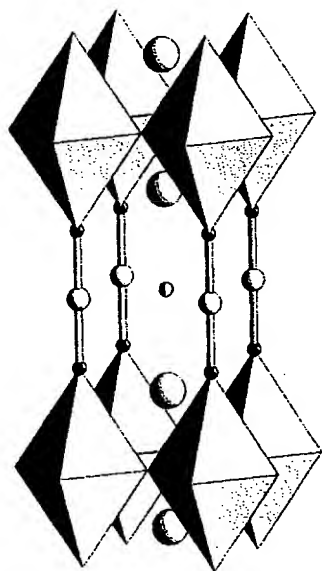


FIG. 3 Structure of $\text{HgBa}_2\text{CuO}_{4+\delta}$. The large, medium and small circles represent the Ba, Hg and O atoms, respectively. The Cu atoms are inside the octahedra. Note that the partially occupied oxygen O(3) site on the Hg layer is represented by a partially filled circle.

pyramidally coordinated. The coordination of the Ba and Hg cations in Hg-1212 is similar to that of the same cations in Hg-1201. The R cations are surrounded by 8 oxygen atoms arranged as a prism. The valence of the Cu cations depends upon the value of δ and the valence of the R cations: if the same Cu valence or hole concentration as in Hg-1201 is needed to induce the superconducting state in Hg-1212, then the R cations should be $2+$ and δ_{1212} should be appreciably greater than δ_{1201} . For the previously reported Hg-1212, R was a mixture of Eu and Ca, and δ was not precisely determined³. It is possible that δ was not large enough to compensate for the higher valence of the R cations and to transfer the needed extra charges to CuO_2 layers.

As stated above, the structural arrangement of $\text{HgBa}_2\text{CuO}_{4+\delta}$ is similar to that of $\text{TlBa}_2\text{CuO}_{4-\delta}$, except for the oxygen stoichiometry of the HgO_8 and $\text{TlO}_{1-\delta}$ layers respectively. For the former, δ is very small and this depletion is possible because the dumb-bell coordination is appropriate for the Hg^{2+} cations. For the latter, the $\text{TlO}_{1-\delta}$ layer is only slightly oxygen depleted, creating the appropriate coordination for the thallium cations, resulting in either a distorted octahedron or a five-coordinated polyhedron. These different requirements for attaining the optimal concentration of holes are due to the different preferred coordination geometries of the Tl^{3+} and Hg^{2+} cations.

The first member of the latter series (Tl-1201) has been reported and found to become superconducting at <10 K (ref. 4). By doping the Ba sites with La this value can be increased to 52 K (ref. 7). The second member of the mono-Tl series becomes superconducting at 85 K (ref. 2). This increase is a general rule for the first few members of this series of compounds. If this behaviour holds for the Hg-series, the second member could reach values for T_c as high as those of the thallium.

The possible advantages for technical applications of $\text{HgBa}_2\text{CuO}_{4+\delta}$, in analogy with one-Tl-layer materials, would be due to the relatively short distance between CuO_2 layers. This might lead to lower anisotropy of the superconducting properties and to higher flux-melting temperatures than those of two-TlO-layer superconductors⁵.

Received 18 December 1992; accepted 12 February 1993.

1. Bednorz, J. G. & Müller, K. A. *Z. Phys.* **B64**, 189–193 (1986).
2. Parkin, S. S. P. et al. *Phys. Rev.* **B38**, 6531–6537 (1988).
3. Putlin, S. N., Bryntse, I. & Antipov, E. V. *Mat. Res. Bull.* **26**, 1299–1307 (1991).
4. Gopalakrishnan, I. K., Yakiml, I. V. & Iyer, R. M. *Physica C* **175**, 183–186 (1991).
5. Kim, D. H. et al. *Physica C* **177**, 431–437 (1991).
6. De Leeuw, O. M., Mutsaers, C. A. H. A., Langeris, C., Smoorenburg, H. C. A. & Rommers, P. J. *Physica C* **152**, 39–49 (1988).
7. Subramanian, M. A., Kwei, G. H., Parise, J. B., Goldstone, J. A. & Von Dreele, R. B. *Physica C* **166**, 19–24 (1990).

ACKNOWLEDGEMENTS. The authors thank R. V. Shpanchenko and J. L. Tholence for their collaboration. S.N.P. thanks O. Massenet for a grant to attend the Laboratoire de Cristallographie of the CNRS, Grenoble. S.N.P. and E.V.A. are supported by grants from the Project "Polak" of the Russian Scientific Council on Superconductivity.

Dependence of aggregate morphology on structure of dimeric surfactants

R. Zana* & Y. Talmon

Department of Chemical Engineering, Technion-Israel Institute of Technology, Haifa 32000, Israel

SURFACTANT molecules in water form organized assemblies of various shapes, such as micelles and bilayer lamellae, which are of interest as analogues of biological structures, as model systems for studying complex phase behaviour and because of their technological importance, for example to the food and paint industries. The polar head groups are usually arranged randomly at the surface of these assemblies. We have studied the effect on the microstructure of these assemblies of imposing constraints on the head-group spacing. We investigate the structures formed by 'double-headed' surfactants in which two quaternary ammonium species ($\text{C}_m\text{H}_{2m+1}\text{N}^+(\text{CH}_3)_2$) are linked at the level of the head groups by a hydrocarbon spacer (C_sH_{2s}). Here we report the microstructures formed by these dimeric surfactants with $m=12$ and $s=2, 3$ or 4 in aqueous solution, by rapidly cooling the micellar solutions and investigating the vitrified structures with transmission electron microscopy. The surfactants with a short spacer ($s=2, 3$) form long, thread-like and entangled micelles even at low concentrations, whereas the corresponding monomeric ammonium surfactants can form only spherical micelles. The dimeric surfactants with $s=4$ form spheroidal micelles. Thus short spacers (which impose reduced head-group separation) appear to promote lower spontaneous curvature in the assemblies. This approach may afford a new way to control amphiphile self-aggregation.

Conventional surfactant molecules generally comprise two distinct parts that are incompatible with each other: one polar head and either one or two alkyl chains. These molecules tend to self-associate in water, where they produce micellar solutions in the dilute range, and lyotropic mesophases at higher concentrations. Whatever the structure, the surfactant polar heads are located at the interface between the hydrocarbon and water regions. Their relative positions and distances are determined mainly by their electrostatic interactions, and also by the packing requirements of the disordered alkyl chains^{1–3}. In caesium or rubidium soaps at low temperature in the presence of water, for example the head groups form well developed hexagonal or rectangular crystalline arrays⁴. Generally, however, they are arranged randomly, and little is known of their packing geometry or the width of their spacing distribution.

To investigate the effect of a perturbation of the local arrangement of polar heads on the micellar and mesomorphic properties

* To whom correspondence should be addressed in Haifa. On leave of absence from Institut Charles Sadron (CNRS), 6 rue Boussingault, 67083 Strasbourg Cedex, France.